### Title

Non-oncogenic Acute Viral Infections Disrupt Anti-cancer Responses and Lead to Accelerated Cancer-Specific Host Death.




### Journal

Cell Reports, 17(4)



### Authors

Kohlhapp, Frederick

Huelsmann, Erica

Lacek, Andrew

et al.



### Publication Date

2016-10-18

### DOI

10.1016/j.celrep.2016.09.068

HHS Public Access

Author manuscript

*Cell Rep*. Author manuscript; available in PMC 2017 September 07.

Published in final edited form as:

*Cell Rep*. 2016 October 18; 17(4): 957–965. doi:10.1016/j.celrep.2016.09.068.

# Non-oncogenic acute viral infections disrupt anti-cancer responses and lead to accelerated cancer-specific host death

**Frederick J. Kohlhapp**[1,2,11], **Erica J. Huelsmann**[3,11], **Andrew T. Lacek**[3,11], **Jason M. Schenkel**[4,11], **Jevgenijs Lusciks**[3,5], **Joseph R. Broucek**[6], **Josef W. Goldufsky**[3], **Tasha Hughes**[6], **Janet P. Zayas**[3], **Hubert Dolubizno**[3], **Ryan T. Sowell**[3], **Regina Kühner**[3], **Sarah Burd**[7], **John C. Kubasiak**[6], **Arman Nabatiyan**[3,5], **Sh'Rae Marshall**[1], **Praveen K. Bommareddy**[1], **Shengguo Li**[1], **Jenna H. Newman**[1], **Claude E. Monken**[1,2], **Sasha H. Shafikhani**[3], **Amanda L. Marzo**[3,5], **Jose A. Guevara-Patino**[8], **Ahmed Lasfar**[1,9], **Paul G. Thomas**[10], **Edmund C. Lattime**[1,2], **Howard L. Kaufman**[1,2], and **Andrew Zloza**[1,2,*]

[1]Division of Surgical Oncology Research, Section of Surgical Oncology, Rutgers Cancer Institute of New Jersey, New Brunswick, NJ, 08903, USA

[2]Department of Surgery, Rutgers Robert Wood Johnson Medical School, New Brunswick, NJ, 08903, USA

[3]Department of Immunology/Microbiology, Rush University Medical Center, Chicago, IL, 60612, USA

[4]Department of Microbiology and Immunology, University of Minnesota, Minneapolis, MN, 55455, USA

[5]Department of Internal Medicine, Rush University Medical Center, Chicago, IL, 60612, USA

[6]Department of General Surgery, Rush University Medical Center, Chicago, IL, 60612, USA

[7]University of Oxford, Oxford, United Kingdom

[8]Department of Surgery, Immunology Institute, Cardinal Bernardin Cancer Center, Loyola University Chicago, Maywood, IL, 60153, USA

[9]Department of Pharmacology and Toxicology, Ernest Mario School of Pharmacy, Rutgers, The State University of New Jersey, Piscataway, NJ, 08854, USA

[10]Department of Immunology, St. Jude Children's Research Hospital, Memphis, TN, 38105, USA

[*]Correspondence/Lead Contact: andrew.zloza@rutgers.edu.

[11]Co-first author



**AUTHOR CONTRIBUTIONS**

A.Z. conceived the project. E.J.H. and A.T.L. performed influenza-related experiments. F.J.K. and J.M.S. designed and analyzed experiments. A.N., R.T.S., S.H.S., A.M., J.A.G-P., A.L., P.G.T., E.C.L. and H.L.K. offered expertise to various components of the project. E.L., J.R.B., T.H., J.P.Z., H.D., R.K., S.B., J.K., S.M., P.B., and S.L. contributed to influenza- and/or LCMV-related experiments. J.G. performed and S.H.S. analyzed *Staphylococcus*-related experiments. C.E.M., J.N., and S.L. performed and analyzed vaccinia virus-related experiments. F.J.K. and A.Z. wrote the manuscript and all authors contributed to writing and/or providing feedback.

## SUMMARY

In light of increased cancer prevalence and cancer-specific deaths in patients with infections, we investigated whether infections alter anti-tumor immune responses. We report that acute influenza infection of the lung promotes distal melanoma growth in the dermis and leads to accelerated cancer- specific host death. Further, we show that during influenza infection anti-melanoma CD8+ T cells are shunted from the tumor to the infection site, where they express high levels of the inhibitory receptor, PD-1. Immunotherapy to block PD-1 reverses this loss of anti- tumor CD8+ T cells from the tumor and decreases infection-induced tumor growth. Our findings show that acute non-oncogenic infection can promote cancer growth, raising concerns regarding acute viral illness sequelae. They also suggest a role for PD-1 blockade in cancer immunotherapy, and provide insight into the immune response when faced with concomitant challenges.


## Graphical abstract

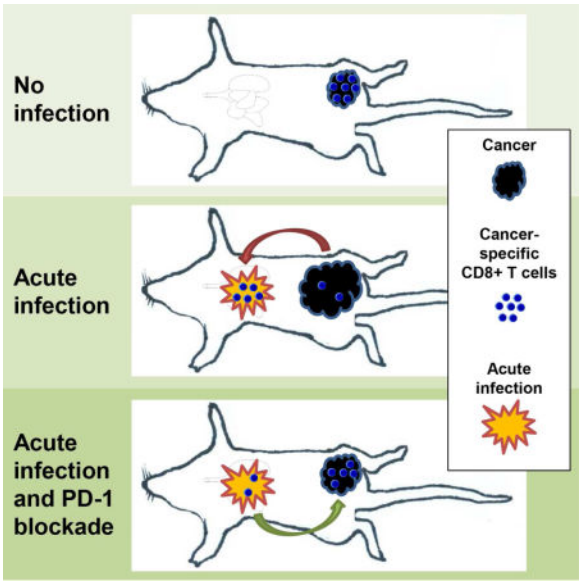


## INTRODUCTION

Our current understanding of immunity relies principally on studies in which a single type of challenge or re-challenge is made to the immune system. Such work has been instrumental in deconstructing complicated immune cell functions and intricate molecular signaling networks. However, the immune system is often tasked with responding to multiple concomitant challenges, and how one type of challenge dictates the immune response to another is not well understood.

The majority of the work thus far on concomitant challenges has been done in the context of pathogenic co-infections, and findings in this field are discordant (Kenney et al., 2015; Mueller et al., 2007; Osborne et al., 2014; Stelekati et al., 2014). Further, although infections and cancers are two of the most common human maladies and cancer patients are at increased risk of infections, very little information is available regarding the consequences

of concomitant non-oncogenic infection and cancer, and thus this subject is a matter of ongoing debate (Cooksley et al., 2005; Kohler et al., 1990; Wong et al., 2010). Case studies performed in the late 19th century report cancer regression in the context of infection-like reactions (*e.g.*, in response to Coley's toxin), and recent work proposes that anti-tumor T cell populations can be expanded as a byproduct of infection (Coley, 1891; Garrett, 2015; Iheagwara et al., 2014). However, emerging epidemiological studies report an increased prevalence of cancers and increased cancer-specific death in patients with infection (Attie et al., 2014; Cox et al., 2010; Crum-Cianflone et al., 2009; Huang et al., 2013; Su et al., 2011; Swaminathan et al., 2015).

Therefore, towards advancing the scientific understanding of immunity in the context of multiple concomitant challenges, we investigated the effect of acute, non-oncogenic, non-immune-destructive infection in one tissue on anti-cancer immune responses in a distal tissue. Surprisingly, we uncovered a potentially common mechanism of immune disruption in cancer-bearing hosts, namely the shunting of anti-tumor CD8+ T cells from the tumor microenvironment to the site of infection by acute non-oncogenic pathogens, an unexpected mechanism of PD-1 blockade in the treatment of cancer, and an unexpected perspective to our basic understanding of the immune response in the context of concomitant challenges.

## RESULTS AND DISCUSSION

### Acute influenza infection leads to accelerated cancer-specific host death

To determine the impact of viral infection on cancer-specific mortality, we inoculated B6 mice with influenza three days prior to distal tumor challenge with B16 melanoma (Figure 1A). Influenza infection significantly accelerated cancer-specific host death ($P<0.001$; Figure 1A). Further, influenza infection as many as 30 days prior to tumor challenge likewise accelerated host death, albeit to a smaller degree compared to infection three days prior to tumor challenge (Figure 1B). Cancer-specific mortality was similar in mice infected and not infected with influenza 60 days prior to tumor challenge (Figure 1C). These data demonstrate that acute influenza infection leads to accelerated cancer-specific host death.

### Influenza infection accelerates the death of hosts with established tumors and leads to the emergence of otherwise controlled tumors

To determine whether influenza similarly affects established tumor growth, mice were challenged with B16 melanoma and then infected three days or seven days later with influenza. Here, influenza infection of hosts with established tumors likewise accelerated cancer-specific host death (Figure 1D).

To determine whether infection could lead to the emergence of cancer that is otherwise controlled by the immune system, we challenged mice with suboptimal cell numbers of B16 (12,000 and 1,200) at which the percentage of tumor-free mice is increased (to 60% and 100%, respectively) compared to our optimal challenge with 120,000 cells (Figure 1E). Here, influenza infection significantly decreased the percentage of tumor-free mice at both 12,000 and 1,200 B16 cell challenges to 0% ($P<0.01$ and $P<0.001$, respectively; Figure 1E).

These data show that concomitant influenza accelerates the death of hosts with established tumors and leads to the emergence of otherwise controlled tumors.

## Infection-accelerated tumor growth and host death occurs in the context of various pathogens and cancers

To determine whether these findings are more broadly applicable, we challenged mice with a series of pathogens, administered through different sites of infection and via varying routes of delivery. Acute LCMV (Armstrong strain) infection, which infects the spleen, liver, and kidneys and is administered via intraperitoneal injection (Ahmed et al., 1984), results in significantly accelerated host death ($P<0.001$; Figure 2A). Further, this phenomenon is not restricted to viruses, since concomitant bacterial infection with *Staphylococcus aureus* also hastened tumor growth ($P<0.05$; Figure 2B). These findings are not restricted to transplantable tumor models, since in a genetically driven mouse model of melanoma (utilizing heterozygous Braf/PTEN mice), increased melanoma was observed in mice infected with influenza and complete penetrance was observed when tamoxifen and influenza were combined (Figure 2C). To assess whether the results observed are applicable to a cancer of another type, in a different tissue, and in a different mouse strain, we determined the effects of influenza infection on 4T1 breast cancer in the mammary fat pad of Balb/c mice. Here, influenza infection significantly increased tumor growth ($P<0.05$) (Figure 2D). Collectively, these data show that infection-accelerated tumor growth and host death occur in the context of various 1) tumor types, 2) sites of tumor challenge, 3) mouse strains, 4) infectious agents, 5) sites of infection, and 6) models of tumor induction.

## Anti-tumor CD8+ T cells are shunted to the lung during influenza infection

CD8+ T cells are important mediators of immunity, tasked with clearing both viral infections and tumors. Therefore, to elucidate the mechanism by which influenza infection promotes tumor growth and reduces survival, we determined the proportion of anti-tumor CD8+ T cells within the tumor and at the infection site. To track anti-tumor CD8+ T cells, we adoptively transferred Thy1.1+ Pmel CD8+ T cells specific against melanoma $gp100_{25–33}$ into Thy1.1− B6 mice (Figure 3A). Surprisingly, in mice infected with influenza, Pmel CD8+ T cells were significantly reduced on day 6 in the tumor compared to uninfected hosts ($P<0.01$) and found at high levels at the site of infection; $P<0.001$; Figure 3B,C). Similar findings were observed in terms of Pmel CD8+ T cell numbers in the tumor and lungs (Figure 3D), but not observed in tissues unrelated to the tumor challenge or infection (Figure 3E).

To determine if anti-tumor CD8+ T cells could traffic from the tumor to the influenza-infected lungs, we transplanted tumors from uninfected B16 melanoma-bearing B6 mice (that previously received an adoptive transfer of Pmel CD8+ T cells) to naïve B6 mice that were subsequently influenza-infected or left uninfected (Figure 3F). Influenza infection resulted in the significant accumulation of tumor-specific (Pmel) CD8+ T cells from the transplanted tumors in the influenza-infected lungs ($P<0.01$) but not spleen (Figure 3G). This finding shows that anti-tumor CD8+ T cells are shunted by a distal infection from the tumor to the site of infection.

### Disruption of anti-tumor responses is not due to tumor-induced immune suppression of viral clearance or inability of the immune system to respond to concomitant challenges

To assess whether the observed disruption of anti-tumor responses leading to accelerated cancer-specific death is due to tumor-induced immune suppression, we inoculated two groups of B6 mice with influenza and challenged one of those groups with distal B16 melanoma. Notably, tumor challenge did not suppress the immune clearance of influenza (Supplemental Figure S1A), demonstrating that cancer in these hosts does not significantly suppress the anti-viral response.

To determine whether accelerated cancer-specific death is due to a general inability of the immune system to respond to concomitant challenges, we infected B6 mice on day −3 with influenza, and/or with vaccinia virus (VACV). Importantly, influenza infection did not alter the natural clearance of VACV (Supplemental Figure S1B) or the proportion of VACV-tetramer+ CD8+ T cells at the site of influenza infection (Supplemental Figure S1C,D), suggesting that influenza infection does not in general prevent concomitant disease clearance, but does accelerate tumor growth in our studies.

### Therapeutic blockade of PD-1 results in reversal of infection-mediated anti-tumor response disruption

Based on the extended period of time necessary after infection clearance for anti-tumor immune responses to be recovered (Figure 1B and C), we hypothesized that infection leads to the dysfunction of anti-tumor CD8+ T cells shunted to the site of infection. Since exhaustion is a hallmark of dysfunctional anti-tumor CD8+ T cells (Ahmadzadeh et al., 2009; Sakuishi et al., 2010; Wherry et al., 2007), we determined the expression of activation and exhaustion receptor, PD-1, on tumor-specific CD8+ T cells. Although PD-1 expression was observed on anti-tumor Pmel CD8+ T cells in the tumor (10–20%; personal observation), a greater proportion of anti-tumor CD8+ T cells expressed PD-1 in the infected lung even when compared to influenza-OVA infection-specific (OT-I) CD8+ T cells in the lungs ($P<0.01$) (Figure 4A–C). Based on this finding and the use of PD-1 blockade in the clinical treatment of melanoma (Hamid et al., 2013), lung cancer (Rizvi et al., 2015), and prostate cancer (Topalian et al., 2012), we investigated whether such systemic blockade in the context of influenza infection would lead to recovered anti-tumor CD8+ T cell responses in the tumor. PD-1 blockade (on days 0 and 2; 100 μg/mouse/day) decelerated tumor growth in influenza-infected mice to the rate observed in untreated uninfected mice (Figure 4D). Further, PD-1 blockade rescued the percentage of anti-tumor CD8+ T cells within the tumor (Figure 4E and F). These data demonstrate that anti-tumor CD8+ T cells shunted to the site of infection upregulate activation and exhaustion marker, PD-1, and that its therapeutic blockade results in reversal of the acceleration of tumor growth by infection.

### Conclusion

Overall, our findings demonstrate that acute, non-oncogenic infection of an unrelated tissue (*i.e.*, distal to the tumor site) results in accelerated tumor growth and hasted host death from cancer. Based on our observations, a mechanism by which infection impedes anti-tumor responses includes the shunting of anti-tumor CD8+ T cell responses from the tumor to the site of infection. The exact means by which this occurs may involve non-specific CD8+ T

cell trafficking to another (or greater) site of inflammation (*e.g.*, via a chemokine gradient), where tumor-specific CD8+ T cells become hyper-activated or exhausted (as illustrated by increased PD-1 expression at the site of infection) and are unable to aid in the immune response at the tumor site. Recent studies demonstrating antigen epitopes shared between some infections and cancers (Snyder et al., 2014) may also explain the observed shunting of CD8+ T cells from the tumor to the infection site. Further, mechanisms yet to be determined may be involved in driving the decision-making process of the immune system in the context of concomitant challenges.

Our findings define a previously unrecognized and potentially common mechanism of immune disruption in cancer-bearing hosts, namely acute non-oncogenic viral infection. This finding is important because it raises concerns regarding previously unrecognized sequelae of acute viral illness, it highlights an unexpected mechanism of PD-1 blockade in the treatment of cancer, it may explain epidemiological findings describing increased cancer prevalence and cancer-specific deaths in the context of infection, and it contributes to our basic understanding of the immune response in the context of concomitant challenges.

## EXPERIMENTAL PROCEDURES

### Mice and adoptive cell transfers

C57BL/6 (B6; #00664), Balb/c (#00651), Braf/PTEN (#13590), Pmel (#5023), and OT-1 (#03831) mice, age 6–8 weeks from Jackson Laboratory, were housed in a specific pathogen-free facility at Rutgers Cancer Institute of New Jersey and/or Rush University Medical Center. Experiments involving animals were carried out in accordance respective Institutional Animal Care and Use Committee and Institutional Biosafety Committee guidelines. Pmel (50,000) and OT-1 (50,000) cells were derived from the spleen and adoptively transferred via injection in 100 μl of PBS into the retroorbital venous sinus.

### Tumor challenges and monitoring

Mice (5–10 per group per experiment, as described for each experiment) were anesthetized with isoflurane and challenged with B16-F10 (1,200–120,000 cells, as described for each experiment) via intradermal injection in the right flank or 4T1-Luciferase (100,000 cells) via injection in the mammary fat pad, as previously described (Bellavance et al., 2011; Kohlhapp et al., 2012; Zloza et al., 2012). Prior to injection, these cells were cultured in RPMI plus 10% heat-inactivated FBS (Atlanta Biologicals), 2 mM L-glutamine (Mediatech), and 1% penicillin/streptomycin (Mediatech). Tumor area (length × width) was measured using calipers. Survival of tumor-bearing mice was defined by tumor size <100 $mm^2$, unless otherwise noted. For 4T1-luciferase experiments, mice were injected with 150 μg D-Luciferin (Sigma-Aldrich) in PBS, anesthetized with isoflurane, and imaged live with the IVIS system (Xenogen), as per manufacturer instructions. For experiments involving Braf/PTEN mice, tumors were induced in some mice using 4HT (1 mg) via intravenous (i.v.) injection (Dankort et al., 2009). For these experiments, all mice were 8 weeks old and were considered to be melanoma-positive if one or more dermal melanomas were observed at day 60. In some experiments, tumors, spleens, and/or lungs were obtained.

### Tumor transplantation experiments

For tumor transplantation experiments, naïve B6 mice (hereafter termed “donor mice”; Thy1.1−) received an adoptive transfer of Pmel CD8+ T cells (into the retroorbital venous sinus; 50,000 cells; Thy1.1+) on day −5 and challenged on day 0 with B16 melanoma (intradermal injection; 120,000 cells). On day 12, B16 tumors (with infiltrating Thy1.1+ Pmel CD8+ T cells) were dissected from donor B6 mice and transplanted into the flank intradermal space (equal size) of a pair (i.e., two) of tumor-free B6 mice (“recipient mice”; Thy1.1−). On day 17, one mouse of each recipient pair was left uninfected [control; PBS administration], and the other mouse of each recipient pair received influenza infection (10,000 pfu via intranasal administration). On day 25, all recipient mice were euthanized and lungs were dissected.

### Infections and PD-1 blockade

For influenza infections, mice were inoculated (10,000 pfu in 40 μl) with influenza A/H1N1/PR8 or influenza-OVA (A/H1N1/PR8-OVA) via intranasal administration (Rutigliano et al., 2014). For LCMV infections, mice were inoculated with LCMV Armstrong strain ($2\times10^5$ pfu) by intraperitoneal (i.p.) injection. For *Staphylococcus aureus* (strain COL) skin infections, a 5-mm biopsy punch was used to create four full thickness wounds in the dorsal skin of mice, opposite from the ventral site of the tumor (Kroin et al., 2015). *Staphylococcus aureus* was applied to the wounds ($1\times10^7$ cfu in 10 μL PBS). Mice were housed in individual cages after wounding to prevent cross-contamination. For vaccinia virus (VACV) skin infections, B6 mice were inoculated with VACV (NYCBH strain) via intradermal (i.d.) injection ($10^6$ PFU) and analyzed by plaque assays (Zhang et al., 2006). For PD-1 blockade, anti-PD-1 (clone RMP1–14; BioXCell; 250 μg) or matched IgG control antibody was administered via i.p. injection.

### Flow cytometry and staining

Cell staining data were collected with the Canto II flow cytometer (BD) and analyzed with FlowJo software (Tree Star) as previously described (Zloza et al., 2012) and tissue-parenchyma (i.e., non-vascular) cells were identified by *in vivo* antibody labeling of cells within the vasculature (Anderson et al., 2014). All antibodies were purchased from eBiosciences.

### Statistical Analysis

Kaplan-Meier curves were used to present animal survival and tumor incidence data and log rank test was used to compare such curves. Unless otherwise noted, student’s t test (two-tailed) was used. All analyses were performed using Prism software (v4.0, GraphPad). A P value of less than 0.05 was considered to denote statistically significant differences.

## Supplementary Material

Refer to Web version on PubMed Central for supplementary material.

## Acknowledgments

We thank the laboratory of J. Pratap (Rush University) for assistance with live animal imaging and the laboratory of A. Chervonsky (The University of Chicago) for assistance with LCMV infection. We thank L. Al-Harthi (Rush University), L. Denzin, and H. Sabaawy (Rutgers, The State University of New Jersey), and J. Rudra (University of Texas, Medical Branch) for helpful discussions and/or manuscript review. This work was supported by grants from the American Cancer Society-Illinois (ORA #13071901-CT01 to A. Z.), Brian Piccolo Cancer Research Fund (to A.Z.), and Bears Care (to S.H.S. and A.Z.) and utilized shared resources at Rutgers Cancer Institute of New Jersey supported by NCI P30CA72720.

## References

Ahmadzadeh M, Johnson LA, Heemskerk B, Wunderlich JR, Dudley ME, White DE, Rosenberg SA. Tumor antigen-specific CD8 T cells infiltrating the tumor express high levels of PD-1 and are functionally impaired. Blood. 2009; 114:1537–1544. [PubMed: 19423728]

Ahmed R, Salmi A, Butler LD, Chiller JM, Oldstone MB. Selection of genetic variants of lymphocytic choriomeningitis virus in spleens of persistently infected mice. Role in suppression of cytotoxic T lymphocyte response and viral persistence. The Journal of experimental medicine. 1984; 160:521–540. [PubMed: 6332167]

Anderson KG, Mayer-Barber K, Sung H, Beura L, James BR, Taylor JJ, Qunaj L, Griffith TS, Vezys V, Barber DL, Masopust D. Intravascular staining for discrimination of vascular and tissue leukocytes. Nat Protoc. 2014; 9:209–222. [PubMed: 24385150]

Attie R, Chinen LT, Yoshioka EM, Silva MC, de Lima VC. Acute bacterial infection negatively impacts cancer specific survival of colorectal cancer patients. World journal of gastroenterology: WJG. 2014; 20:13930–13935. [PubMed: 25320529]

Bellavance EC, Kohlhapp FJ, Zloza A, O'Sullivan JA, McCracken J, Jagoda MC, Lacek AT, Posner MC, Guevara-Patino JA. Development of tumor-infiltrating CD8+ T cell memory precursor effector cells and antimelanoma memory responses are the result of vaccination and TGF-beta blockade during the perioperative period of tumor resection. Journal of immunology. 2011; 186:3309–3316.

Coley WB. II. Contribution to the Knowledge of Sarcoma. Annals of surgery. 1891; 14:199–220.

Cooksley CD, Avritscher EB, Bekele BN, Rolston KV, Geraci JM, Elting LS. Epidemiology and outcomes of serious influenza-related infections in the cancer population. Cancer. 2005; 104:618–628. [PubMed: 15973737]

Cox B, Richardson A, Graham P, Gislefoss RE, Jellum E, Rollag H. Breast cancer, cytomegalovirus and Epstein-Barr virus: a nested case-control study. British journal of cancer. 2010; 102:1665–1669. [PubMed: 20407437]

Crum-Cianflone N, Hullsiek KH, Marconi V, Weintrob A, Ganesan A, Barthel RV, Fraser S, Agan BK, Wegner S. Trends in the incidence of cancers among HIV-infected persons and the impact of antiretroviral therapy: a 20-year cohort study. Aids. 2009; 23:41–50. [PubMed: 19050385]

Dankort D, Curley DP, Cartlidge RA, Nelson B, Karnezis AN, Damsky WE Jr, You MJ, DePinho RA, McMahon M, Bosenberg M. Braf(V600E) cooperates with Pten loss to induce metastatic melanoma. Nature genetics. 2009; 41:544–552. [PubMed: 19282848]

Garrett WS. Cancer and the microbiota. Science. 2015; 348:80–86. [PubMed: 25838377]

Hamid O, Robert C, Daud A, Hodi FS, Hwu WJ, Kefford R, Wolchok JD, Hersey P, Joseph RW, Weber JS, et al. Safety and tumor responses with lambrolizumab (anti-PD-1) in melanoma. The New England journal of medicine. 2013; 369:134–144. [PubMed: 23724846]

Huang J, Magnusson M, Torner A, Ye W, Duberg AS. Risk of pancreatic cancer among individuals with hepatitis C or hepatitis B virus infection: a nationwide study in Sweden. British journal of cancer. 2013; 109:2917–2923. [PubMed: 24178755]

Iheagwara UK, Beatty PL, Van PT, Ross TM, Minden JS, Finn OJ. Influenza virus infection elicits protective antibodies and T cells specific for host cell antigens also expressed as tumor-associated antigens: a new view of cancer immunosurveillance. Cancer immunology research. 2014; 2:263–273. [PubMed: 24778322]

Kenney LL, Cornberg M, Chen AT, Emonet S, de la Torre JC, Selin LK. Increased Immune Response Variability during Simultaneous Viral Coinfection Leads to Unpredictability in CD8 T Cell Immunity and Pathogenesis. J Virol. 2015; 89:10786–10801. [PubMed: 26269191]

Kohler M, Ruttner B, Cooper S, Hengartner H, Zinkernagel RM. Enhanced tumor susceptibility of immunocompetent mice infected with lymphocytic choriomeningitis virus. Cancer immunology, immunotherapy: CII. 1990; 32:117–124. [PubMed: 2289203]

Kohlhapp FJ, Zloza A, O'Sullivan JA, Moore TV, Lacek AT, Jagoda MC, McCracken J, Cole DJ, Guevara-Patino JA. CD8(+) T cells sabotage their own memory potential through IFN-gamma-dependent modification of the IL-12/IL-15 receptor alpha axis on dendritic cells. Journal of immunology. 2012; 188:3639–3647.

Kroin JS, Buvanendran A, Li J, Moric M, Im HJ, Tuman KJ, Shafikhani SH. Short-term glycemic control is effective in reducing surgical site infection in diabetic rats. Anesthesia and analgesia. 2015; 120:1289–1296. [PubMed: 25695673]

Mueller SN, Hosiawa-Meagher KA, Konieczny BT, Sullivan BM, Bachmann MF, Locksley RM, Ahmed R, Matloubian M. Regulation of homeostatic chemokine expression and cell trafficking during immune responses. Science. 2007; 317:670–674. [PubMed: 17673664]

Osborne LC, Monticelli LA, Nice TJ, Sutherland TE, Siracusa MC, Hepworth MR, Tomov VT, Kobuley D, Tran SV, Bittinger K, et al. Coinfection. Virus-helminth coinfection reveals a microbiota-independent mechanism of immunomodulation. Science. 2014; 345:578–582. [PubMed: 25082704]

Rizvi NA, Mazieres J, Planchard D, Stinchcombe TE, Dy GK, Antonia SJ, Horn L, Lena H, Minenza E, Mennecier B, et al. Activity and safety of nivolumab, an anti-PD-1 immune checkpoint inhibitor, for patients with advanced, refractory squamous non-small-cell lung cancer (CheckMate 063): a phase 2, single-arm trial. The Lancet Oncology. 2015; 16:257–265. [PubMed: 25704439]

Rutigliano JA, Sharma S, Morris MY, Oguin TH 3rd, McClaren JL, Doherty PC, Thomas PG. Highly pathological influenza A virus infection is associated with augmented expression of PD-1 by functionally compromised virus-specific CD8+ T cells. J Virol. 2014; 88:1636–1651. [PubMed: 24257598]

Sakuishi K, Apetoh L, Sullivan JM, Blazar BR, Kuchroo VK, Anderson AC. Targeting Tim-3 and PD-1 pathways to reverse T cell exhaustion and restore anti-tumor immunity. The Journal of experimental medicine. 2010; 207:2187–2194. [PubMed: 20819927]

Snyder A, Makarov V, Merghoub T, Yuan J, Zaretsky JM, Desrichard A, Walsh LA, Postow MA, Wong P, Ho TS, et al. Genetic basis for clinical response to CTLA-4 blockade in melanoma. The New England journal of medicine. 2014; 371:2189–2199. [PubMed: 25409260]

Stelekati E, Shin H, Doering TA, Dolfi DV, Ziegler CG, Beiting DP, Dawson L, Liboon J, Wolski D, Ali MA, et al. Bystander chronic infection negatively impacts development of CD8(+) T cell memory. Immunity. 2014; 40:801–813. [PubMed: 24837104]

Su FH, Chang SN, Chen PC, Sung FC, Su CT, Yeh CC. Association between chronic viral hepatitis infection and breast cancer risk: a nationwide population-based case-control study. BMC cancer. 2011; 11:495. [PubMed: 22115285]

Swaminathan S, Klemm L, Park E, Papaemmanuil E, Ford A, Kweon SM, Trageser D, Hasselfeld B, Henke N, Mooster J, et al. Mechanisms of clonal evolution in childhood acute lymphoblastic leukemia. Nature immunology. 2015; 16:766–774. [PubMed: 25985233]

Topalian SL, Hodi FS, Brahmer JR, Gettinger SN, Smith DC, McDermott DF, Powderly JD, Carvajal RD, Sosman JA, Atkins MB, et al. Safety, activity, and immune correlates of anti-PD-1 antibody in cancer. The New England journal of medicine. 2012; 366:2443–2454. [PubMed: 22658127]

Wherry EJ, Ha SJ, Kaech SM, Haining WN, Sarkar S, Kalia V, Subramaniam S, Blattman JN, Barber DL, Ahmed R. Molecular signature of CD8+ T cell exhaustion during chronic viral infection. Immunity. 2007; 27:670–684. [PubMed: 17950003]

Wong A, Marrie TJ, Garg S, Kellner JD, Tyrrell GJ, Group S. Increased risk of invasive pneumococcal disease in haematological and solid-organ malignancies. Epidemiology and infection. 2010; 138:1804–1810. [PubMed: 20429967]

Zhang H, Monken CE, Zhang Y, Lenard J, Mizushima N, Lattime EC, Jin S. Cellular autophagy machinery is not required for vaccinia virus replication and maturation. Autophagy. 2006; 2:91–95. [PubMed: 16874104]

Zloza A, Kohlhapp FJ, Lyons GE, Schenkel JM, Moore TV, Lacek AT, O'Sullivan JA, Varanasi V, Williams JW, Jagoda MC, et al. NKG2D signaling on CD8(+) T cells represses T-bet and rescues CD4-unhelped CD8(+) T cell memory recall but not effector responses. Nature medicine. 2012; 18:422–428.

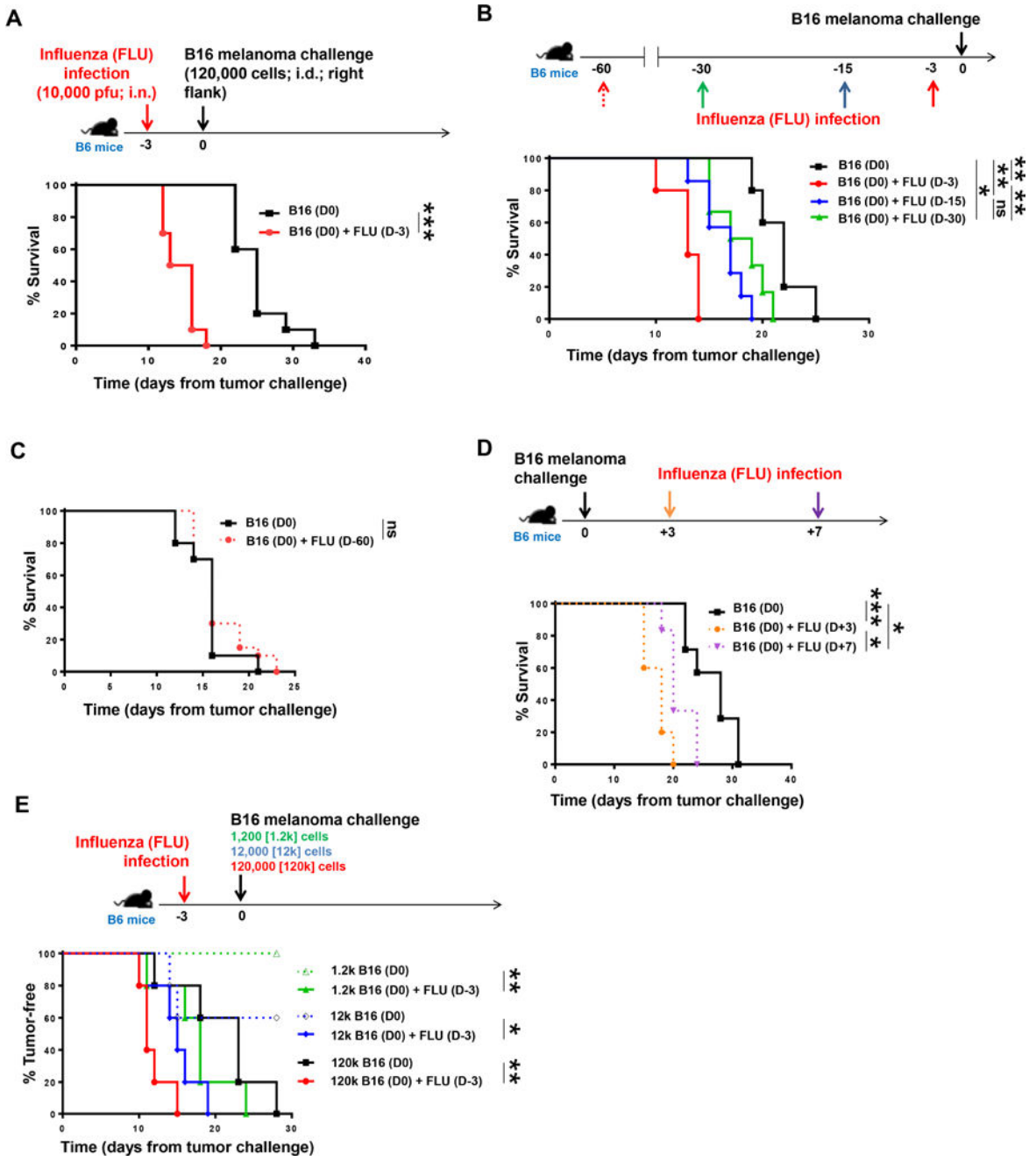


**Figure 1. Influenza infection results in accelerated melanoma-specific host death**

(A) Experimental design (*top panel*). Survival of B6 mice infected on day −3 with influenza and challenged with B16 melanoma on day 0 via intradermal (i.d.) injection (*bottom panel*).

(B) Experimental design (*top panel)*. Survival of B6 mice infected on day −3, −15, or −30 with influenza and challenged with B16 melanoma on day 0 (*bottom panel)*.

(C) Survival of B6 mice infected on day −60 with influenza and challenged with B16 melanoma on day 0.

(D) Experimental design (*top panel*). Survival of B6 mice infected on day +3 or +7 with influenza and challenged with B16 melanoma on day 0 (*bottom panel*).

(E) Experimental design (*top panel)*. Percentage of B6 mice remaining tumor-free after infection on day −3 with influenza and challenge with B16 melanoma (120,000, 12,000 or 1,200 cells) on day 0 (*bottom panel)*.

All experiments were performed with 7–10 mice per group with at least two independent repeat experiments. Survival in (A-E) was defined by tumor size <100 $mm^2$. *, P<0.05; **, P<0.01; ***, P<0.001; ns, not significant.

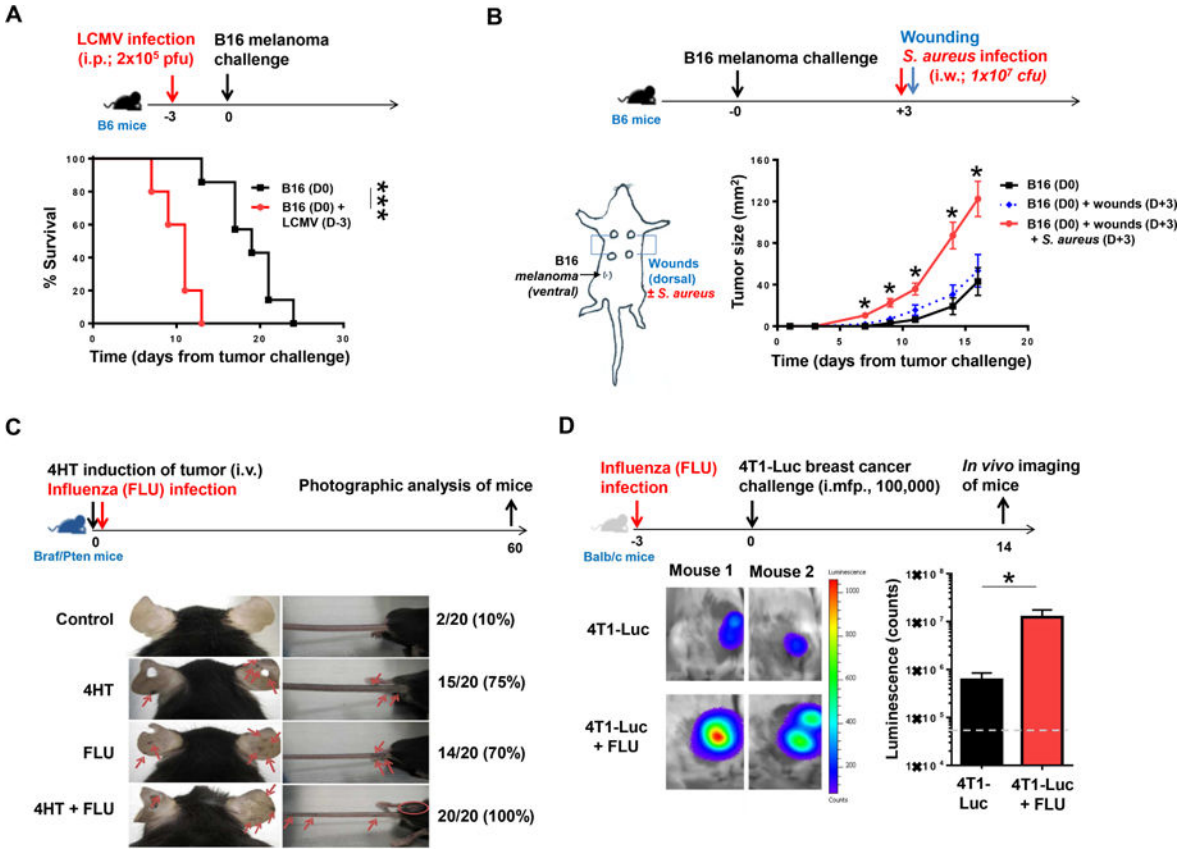


**Figure 2. Pathogenic infections accelerate tumor growth in the context of various cancers**

(A) Experimental design (*top panel*). Survival of B6 mice infected LCMV (Armstrong strain) on day −3 and challenged with B16 melanoma on day 0 via intradermal (i.d.) injection (*bottom panel*). Survival was defined by tumor size <100 $mm^2$.

(B) Experimental design (*top panel*) and wound and infection diagram (*bottom left panel*). Tumor growth in B6 mice challenged with B16 melanoma on day 0, wounded on day +3, and infected at day +3 with *Staphylococcus aureus* via intra-wound (i.w.) injection (*bottom right panel*).

(C) Experimental design (*top panel*). Tumor incidence in Braf/PTEN mice infected at 8 weeks of age with influenza and/or treated with 4HT on day 0. Representative images and number and percentages of mice with one or more observed tumors on day 60 from two combined experiments (*bottom panel*). Red arrows indicate areas of melanoma growth.

(D) Experimental design (*top panel*). Balb/c mice were infected on day −3 with influenza and challenged with 4T1-Luciferase (4T1-Luc) murine breast cancer cells on day 0 via intra-mammary fat pad (i.mfp.) injection. Tumor growth was measured using the live imaging IVIS system (*bottom panel*). Results are depicted with representative luminescence images (*left panel*) and cumulative bar graphs (*right panel*). Dashed lines depict background luminescence.

All experiments were performed with 5–10 mice per group with at least two independent repeat experiments. *, P<0.05; ***, P<0.001; ns, not significant.

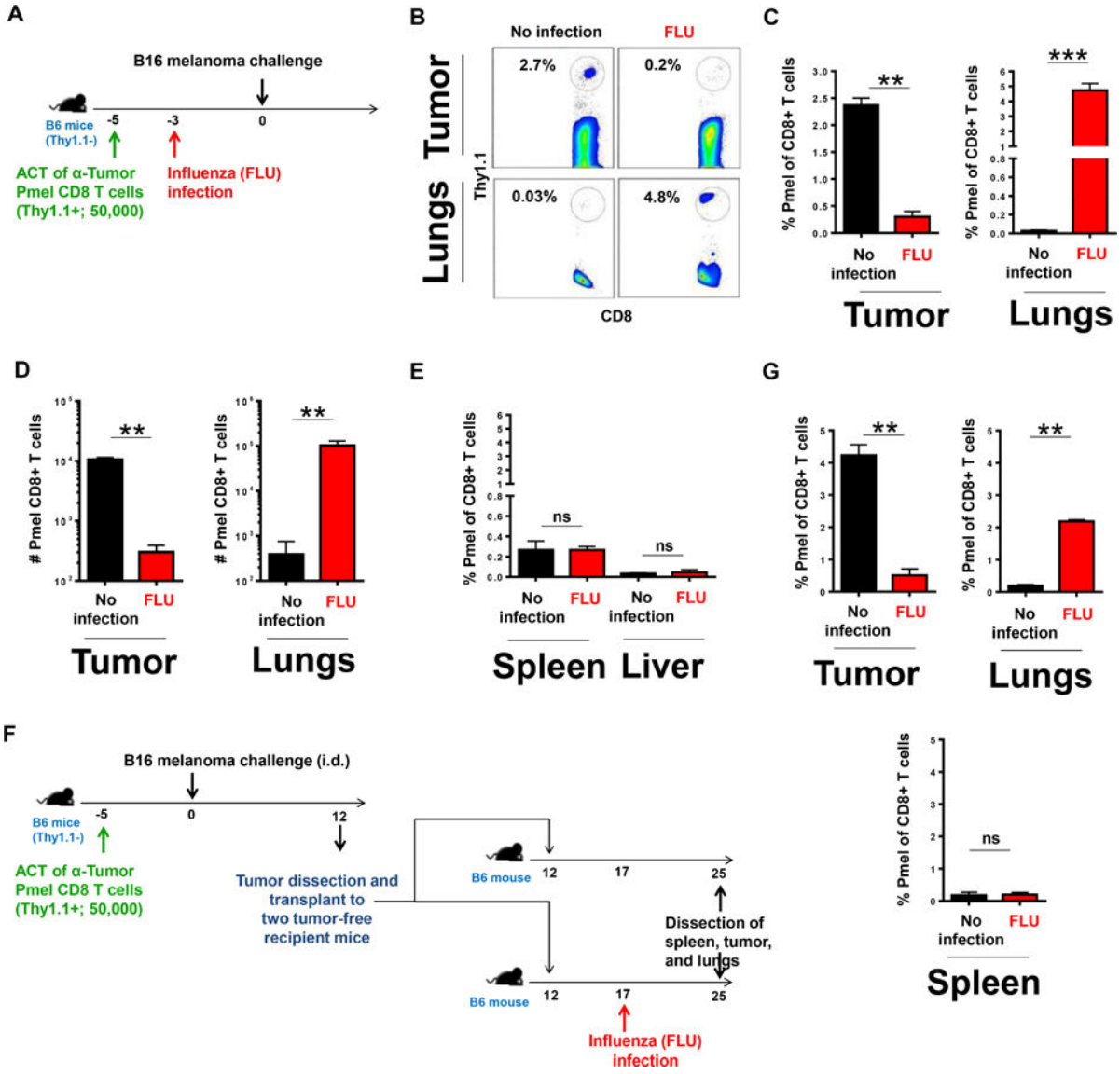


**Figure 3. Melanoma-specific CD8+ T cells are shunted from the tumor to the site of infection**

(A) Experimental design for studies in which B6 mice received adoptive cell transfer (ACT) of Pmel cells on day −5, were infected with influenza on day −3, and were challenged with B16 melanoma on day 0.

(B) Tumors from experiment described in (A) were resected at day 15 and analyzed via flow cytometry. Results depicted by representative flow plots show % of Pmel CD8+ T cells among all CD8+ T cells. Axes on all plots are log scale.

(C) Cumulative bar graphs showing percentage of Pmel CD8+ T cells determined from the experiment described in (A).

(D) Cumulative bar graphs showing number of Pmel CD8+ T cells determined from the experiment described in (A).

(E) Cumulative bar graphs showing percentage of Pmel CD8+ T cells determined from the experiment described in (A).

(F) Experimental design for studies in which B6 mice (Thy1.1−; donor mice) received adoptive cell transfer (ACT) of Pmel cells (Thy1.1+) on day −5 and were challenged with B16 melanoma on day 0. On day 12, each tumor (~36 $mm^2$) was resected and transplanted into the intradermal space of the right flank of two naïve B6 mice (recipient mice). On day 17, one of two naïve B6 tumor-recipient mice from each pair was infected with influenza. (G) Tumor, lungs, and spleen from mice in the experiment described in (F) were resected on day 25 and the presence of Pmel CD8+ T cells was determined by flow cytometry.
All experiments were performed with 5–10 mice per group with at least two independent repeat experiments. **, P<0.01; ***, P<0.001; ns, not significant.

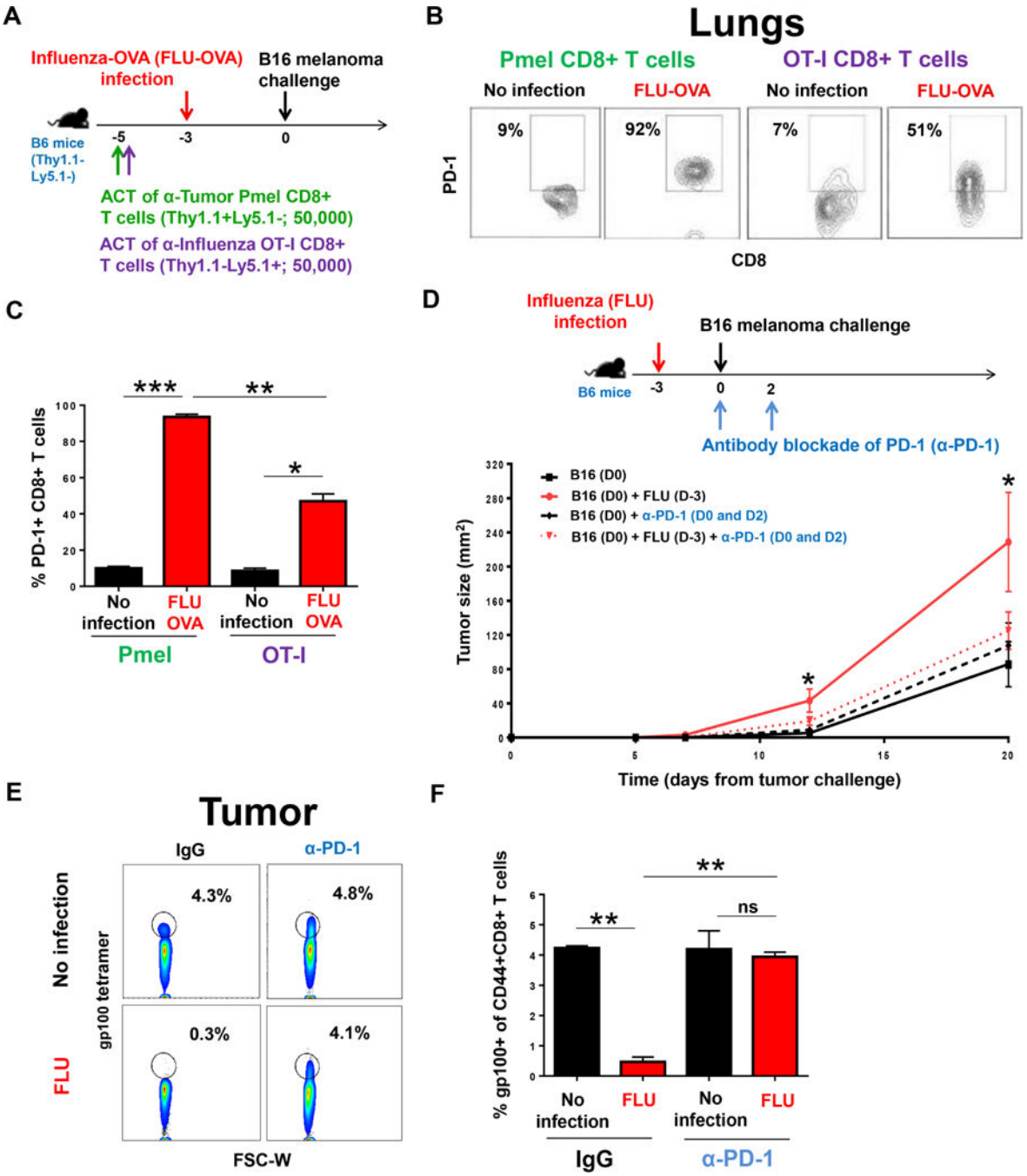


**Figure 4. PD-1 blockade rescues anti-tumor responses impeded by infection**

(A) Experimental design for studies in which B6 mice (Thy1.1−Ly5.1−) received an adoptive cell transfer (ACT) on day −5 of Pmel cells (Thy1.1+Ly5.1−) and OT-I cells (Thy1.1−Ly5.1+) via intravenous (i.v.) injection, were infected on day −3 with influenza-OVA, and challenged with B16 melanoma on day 0.

(B) Lungs from experiment described in (A) were resected at day 10 and PD-1 expression by Pmel and OT-I CD8+ T cells was determined by flow cytometry as shown in representative flow plots. Axes on all plots are log scale.

(C) Cumulative bar graphs showing percentage of Pmel CD8+ T cells determined from the experiment described in (A).

(D) Experimental design (*top panel*). B6 mice were infected with influenza (FLU) at day −3 and challenged with B16 melanoma via intradermal (i.d.) injection. No adoptive transfer of CD8+ T cells was conducted in this experiment. Some mice were treated with PD-1 blocking antibody (anti-PD-1, 100 μg) on days 0 and 2 (*bottom panel*).

(E) Tumors were resected at day 20 and endogenous melanoma-specific CD8+ T cells were identified using $gp100_{25–33}$ tetramer staining after gating on CD8+CD44+ T cells, as shown in the representative flow plots. Y-axis on all plots is log scale, x-axis is linear scale.

(F) Cumulative bar graphs showing % of Pmel CD8+CD44+ T cells determined from the experiment described in (E).

All experiments were performed with 5–10 mice per group with at least two independent repeat experiments. *, $P<0.05$; **, $P<0.01$; ***, $P<0.001$; ns, not significant.